Cerebral Cortex July 2006;16:1030–1039
doi:10.1093/cercor/bhj045
Advance Access publication October 5, 2005

Selective Age-related Degradation of Anterior Callosal Fiber Bundles Quantified *In Vivo* with Fiber Tracking

Edith V. Sullivan[1], Elfar Adalsteinsson[2,3] and Adolf Pfefferbaum[1,4]

[1]Department of Psychiatry and Behavioral Sciences, Stanford University School of Medicine, Stanford, CA 94305, USA, [2]Department of Electrical Engineering and Computer Science, Massachusetts Institute of Technology, Cambridge, MA, USA, [3]Harvard-MIT Division of Health Sciences & Technology, Massachusetts Institute of Technology, Cambridge, MA, USA and [4]Neuroscience Program, SRI International, Menlo Park, CA 94025, USA

The corpus callosum, the principal white matter structure enabling interhemispheric information transfer, is heterogeneous in its microstructural composition, heterotopic in its anteroposterior cortical connectivity, and differentially susceptible to aging. *In vivo* characterization of callosal features is possible with diffusion tensor imaging (DTI), a magnetic resonance imaging method sensitive to the detection of white matter's linear structure. We implemented a quantitative fiber tracking approach to examine age-related variation in regional microstructural characteristics [fractional anisotropy (FA) and apparent diffusion coefficient (ADC)] of callosal fibers in 10 younger (29 ± 5 years) and 10 older (72 ± 5 years) healthy adults. Fiber tracking was performed on 2.5 mm isotropic voxels collected at 3 T. Fiber targets comprised the midsagittal corpus callosum, divided into six regions based on known callosal anatomical projections. FA and ADC for each voxel of each fiber identified were determined; lower FA and higher ADC reflect degraded microstructural tissue integrity. Older subjects had lower FA ($P < 0.002$), higher ADC ($P < 0.006$), and fewer ($P < 0.005$) fibers than younger subjects. Group × region interactions indicated disproportionately lower FA ($P = 0.0001$) and higher ADC ($P < 0.006$) in the older than younger group in frontal fiber bundles relative to posterior bundles. As a test of the functional significance of the fiber bundle metrics, the older subjects were administered the Stroop Task, which showed significant correlations between regional fiber bundle integrity and performance. These results validate this quantitative fiber tracking approach and confirm the selective vulnerability of frontal white matter systems to normal aging, likely substrates of age-related declines in cognitive processes dependent on prefrontal circuitry integrity.

Keywords: aging, apparent diffusion coefficient, corpus callosum, fractional anisotropy, white matter

Introduction

The corpus callosum, the principal white matter structure enabling interhemispheric information transfer (Gazzaniga, 1995), is heterogeneous in its microstructural composition (LaMantia and Rakic, 1990), heterotopic in its anteroposterior cortical connectivity (de Lacoste *et al.*, 1985; Pandya and Seltzer, 1986; Schwartz and Goldman-Rakic, 1991), and differentially susceptible to aging (Aboitiz *et al.*, 1996; Sullivan *et al.*, 2002). *In vivo* characterization of the gross morphology of callosal features modified during aging indicates (at most) modest thinning of its cross-sectional area, measured on midsagittal sections, through young to middle adulthood (Pfefferbaum *et al.*, 1996) with accelerated thinning in older age (Driesen and Raz, 1995; Salat *et al.*, 1997). The age-related thinning is complemented by the contemporaneous expansion of lateral ventricular volume (Pfefferbaum *et al.*, 2000c) and driven, at least in part, by genetic factors determining ventricular size (Pfefferbaum *et al.*, 2004). Gross morphology of the corpus callosum measured on conventional magnetic resonance imaging (MRI), however, does not necessarily reflect the underlying quality of tissue in its microstructure, which is measurable with MR diffusion tensor imaging (DTI) (Moseley *et al.*, 1990; Basser and Pierpaoli, 1996; Pierpaoli and Basser, 1996; Le Bihan, 2003).

By taking advantage of the molecular diffusion of water, the primary constituent of the brain's composition, DTI can detect the microenvironment of white matter and provide assessment of physical characteristics of white matter fibers, which vary widely in length, diameter, and myelination and by region (Waxman *et al.*, 1995). Highly restricted diffusion in a linear framework, such as white matter, has a preferential orientation, is anisotropic, and is typically expressed as fractional anisotropy (FA). By contrast, unrestricted diffusion, as occurs in ventricular space, has no preferential orientation and is isotropic. Diffusivity, expressed as apparent diffusion coefficient (ADC), provides a measure of the amount of water motility (independent of orientation) in a voxel and is commonly but not necessarily negatively correlated with FA within white matter samples (Engelter *et al.*, 2000; Chen *et al.*, 2001; Helenius *et al.*, 2002; Naganawa *et al.*, 2003; Head *et al.*, 2004; Pfefferbaum and Sullivan, 2003, 2005b; Pfefferbaum *et al.*, 2005). Aging, disease or physical trauma can perturb the axon's cytoskeleton and myelin microstructure (Arfanakis *et al.*, 2002), and this disruption can be detected with DTI (Beaulieu and Allen, 1994; Basser and Pierpaoli, 1996; Fenrich *et al.*, 2001; Sehy *et al.*, 2002; Silva *et al.*, 2002; for reviews, see Pfefferbaum and Sullivan, 2005a; Sullivan and Pfefferbaum, 2005).

Post-mortem investigations report that accompanying normal aging is breakdown of myelin and certain constituents of cytoskeleton, reduction in axon density, and decline in the number and length of myelinated fibers (Meier-Ruge *et al.*, 1992; Kemper, 1994; Aboitiz *et al.*, 1996; Marner *et al.*, 2003). A predilection of loss occurs for thin, unmyelinated fibers, which are in greatest abundance in the frontal lobes and genu of the corpus callosum (Aboitiz *et al.*, 1996; Bartzokis, 2004). Consistent with post-mortem studies are findings from *in vivo* neuroimaging studies. In particular, longitudinal studies using conventional MRI report faster volume decline in prefrontal cortical regions relative to posterior cortex in healthy adults (Pfefferbaum *et al.*, 1998; Raz *et al.*, 2005; Resnick *et al.*, 2003). The majority of DTI studies indicate that with advancing age anisotropy declines and diffusivity increases, more notably in anterior than posterior brain regions (Pfefferbaum *et al.*, 2000a;

O'Sullivan *et al.*, 2001; Sullivan *et al.*, 2001; Pfefferbaum and Sullivan, 2003; Head *et al.*, 2004; Madden *et al.*, 2004; Salat *et al.*, 2005); however, one study failed to observe age-related declines in anisotropy in corpus callosum (Chepuri *et al.*, 2002). A profile analysis of white matter across the full extent of the supratentorium revealed that the primary locus of the age effect was in anterior white matter, including the genu of the corpus callosum (Pfefferbaum *et al.*, 2005). Several of these studies in healthy adults also examined the power of DTI metrics as predictors of cognitive or motor performance and observed, for example, that slow reaction time in a visual target detection task correlated with low anisotropy in the anterior limb of the internal capsule (Madden *et al.*, 2004), that low scores on a test of attentional set shifting (Trail Making B-A) correlated with diffusivity in anterior brain regions (O'Sullivan *et al.*, 2001), and that low output on an alternating finger tapping test correlated with low callosal anisotropy (Sullivan *et al.*, 2001).

These DTI studies were based on analyses of intravoxel anisotropy in regionally restricted, white matter samples or, in one case, a profile analysis of supratentorial white matter (Pfefferbaum *et al.*, 2005), but did not take advantage of DTI's ability to depict white matter systems through fiber tracking (e.g. Pierpaoli and Basser, 1996; Tang *et al.*, 1997; Basser, 1998; Conturo *et al.*, 1999; Jones *et al.*, 1999; Mori *et al.*, 2002; Pajevic *et al.*, 2002; Masutani *et al.*, 2003; Lazar and Alexander, 2005). Voxel-to-voxel connectivity between different brain regions is readily apparent on visual fiber tracking displays (Stieltjes *et al.*, 2001; Xu *et al.*, 2002; Lehericy *et al.*, 2004), and measurement of FA and ADC along the length of a fiber bundle renders an estimate of its integrity. This approach, referred to as quantitative fiber tracking, does not actually identify anatomically specific fibers or fiber bundles as detected histologically. Rather, it is a statistical representation of the voxel-to-voxel coherence of MRI-detectable water diffusion in white matter that is, nonetheless, increasingly being shown as representative of the underlying anatomy.

In the present report, using imaging data from our recent publication on supratentorial white matter profile and specific region of interest analysis of age-related differences in DTI metrics (Pfefferbaum *et al.*, 2005), we combined quantitative fiber tracking (cf. Xu *et al.*, 2002) of DTI data based on the method of Mori and van Zijl (2002) and Gerig *et al.* (2005) with structural MRI used as a template for sectioning the corpus callosum into six anatomical regions, based on the histological studies of monkeys by Pandya and Selzer (1986) with consideration from human post-mortem studies (de Lacoste *et al.*, 1985). Because the primary aim of this analysis was to characterize *in vivo* callosal microstructure connecting the cerebral hemispheres, we required that identified 'fibers' span at least 10 mm across both sides of the midline of the corpus callosum. With DTI metrics, we tested the hypothesis that, relative to healthy individuals in their 20s, older healthy individuals in their 70s would have lower anisotropy (FA), higher diffusivity (ADC), shorter fiber length and fewer fibers coursing through the anterior but not posterior sectors of the corpus callosum. As an initial test of the potential functional ramifications of age-related regional compromise of callosal microstructure, we also examined the value of the DTI metrics in predicting performance on the Stroop Color–Word Test (Stroop, 1935). Components of this test may require only unihemispheric processing in young adults (Weekes and Zaidel, 1996; Belanger and Cimino, 2002) but may require bihemispheric processing in older adults (cf. Cabeza, 2002; Cabeza *et al.*, 2002).

Materials and Methods

Subjects

Two groups of healthy, highly educated adults were studied: 10 younger (mean = 28.6, range = 22–37 years, 17.2 years of education; five men, five women) and 10 older (mean = 72.2, range = 65–79 years, 16.3 years of education; five men, five women). The younger subjects included laboratory members and men and women recruited from the local community. All older subjects were recruited from a larger ongoing study of normal aging and scored well within the normal range on dementia screening tests: Mini-Mental State Examination (Folstein *et al.*, 1975), mean = 28.9, range = 27–30 out of 30; and the Dementia Rating Scale (Mattis, 1988), mean = 140.1, range = 138–143 out of 144.

MRI and DTI Acquisition Protocol

The DTI-structural acquisition included a separate acquisition of a field map to be used for correction of spatial distortion due to main field (B_0) inhomogeneity. MRI data were acquired on a 3T General Electric (Milwaukee, WI) Signa human MRI scanner (gradient strength = 40 mT/m; slew rate = 150 T/m/s; software version VH3). Four axial sequences were collected:

1. structural fast spin echo (FSE; FOV = 24 cm, T_R = 10 s, T_E = 14.98 ms, thick = 2.5 mm, skip = 0 mm, slices = 62);
2. Inversion Recovery Prepared SPoiled Gradient Recalled echo (IR-PrepSPGR; FOV = 24 cm, T_I = 300 ms, T_R/T_E = 6.5/1.54 ms, thick = 1.25 mm, slices = 124);
3. Diffusion Tensor Images (DTI; FOV = 24 cm, T_R = 11 000 ms, T_E = 97.6 ms, thick = 2.5 mm, skip = 0, slices = 62, 0 (8 NEX) + 6 non-collinear diffusion directions (4 NEX, gradient orientations $+x+y$, $+y+z$, $+x+z$, $-x+y$, $-y+z$, $+x-z$, with a repeat of these six orientations with opposite gradient polarity, 1.5 Gauss/cm with 32 ms duration and 34 ms separation, resulting in a *b*-value of 860 s/mm^2, *x*-dim = 96, *y*-dim = 96, 3472 total images);
4. fieldmap [FOV = 24 cm, multislice, dual echo, multi-shot (16) spiral acquisition, *x*-dim = 128, *y*-dim = 128].

The SPGR data were aligned such that adjacent pairs of 1.25 mm thick SPGR slices subtended each 2.5-mm-thick FSE and DTI slice using custom scanner prescription software, which computed precise slice locations. The data from the spiral acquisition for each echo were gridded and Fourier transformed, and a fieldmap was estimated from a complex difference image between the two echoes (Glover and Lai, 1998; Pfeuffer *et al.*, 2002).

DTI Analysis

DTI quantification was preceded by eddy current correction on a slice × slice basis by within-slice registration, which takes advantage of the symmetry of the opposing polarity acquisition (Bodammer *et al.*, 2004). The reversing diffusion gradient polarity scheme also allowed for compensation of the diffusion effect created by the imaging gradients by averaging the opposite polarity data (Neeman *et al.*, 1991), reducing the data to six non-collinear diffusion weighted images per slice. Using the field maps, B_0-field inhomogeneity induced geometric distortion in the eddy current-corrected images was corrected with PRELUDE (Phase Region Expanding Labeller for Unwrapping Discrete Estimates; Jenkinson, 2003) and FUGUE (FMRIB's Utility for Geometrically Unwarping EPIs; http://www.fmrib.ox.ac.uk/fsl/fugue/). These 'native' DTI data were used for fiber tracking.

Warping to Common Coordinates

To place the images for all subjects into a coordinate system with a common origin and a standardized anatomical orientation, the anterior commissure (AC) and posterior commissure (PC) were manually identified on the native 1.25-mm-thick SPGR images. The AC was shifted to a fixed coordinate in the anterior/posterior orientation, and the image volume was oriented by three rotations with the AC as the pivot point. After this shift and rotations, the original oblique-axial plane that

passed through the AC and PC was a straight axial section perpendicular to the midsagittal plane. Next, a grand average SPGR data set was created from all 20 subjects. This average was then used as a template upon which each subject was aligned (individual SPGR to template SPGR) with a 12-parameter affine model, followed by creation of a new grand average used as a template for a higher-order (third to fifth polynomial) nonlinear warp. The use of nonlinear warping allowed the registration of young and old brains to a common space despite age-related differences in morphology; for instance, of the corpus callosum that expands in height and length with age (Pfefferbaum *et al.*, 2000c). Two iterations of alignment produced the grand average SPGR image. The early echo FSE data for each subject were then aligned to the SPGR grand average with AIR5.2.5 (http://bishopw.loni.ucla.edu/AIR5/index.html; Woods *et al.*, 1998a,b) using the standard-deviation-of-ratio-image cost function, followed by higher-order (third to fifth polynomial) nonlinear warp, resliced in the native coordinates (1.875 mm isotropic voxels) and an FSE grand average was also created. Next the $b = 0$ images were warped to the native late echo FSE images in three dimensions, first with a 12 parameter affine, followed by stepwise second and third order polynomial functions. Finally, for each subject all the registration transformation matrices were then combined into one function so they could be applied only once to native data. This process allowed for anatomical identification of the corpus callosum in a common space for each subject from structural or FA images and the DTI data to be accessed either in native or common space.

From the $b = 0$ and six diffusion weighted images, six maps of the apparent diffusion coefficient (ADC) were calculated. Solving six simultaneous equations with respect to ADC*xx*, ADC*xy*, etc. yielded the elements of the diffusion tensor. The diffusion tensor was then diagonalized, yielding eigenvalues λ_1, λ_2, λ_3, as well as eigenvectors that define the predominant diffusion orientation. Based on the eigenvalues, FA and ADC were calculated on a voxel × voxel basis (Pierpaoli and Basser, 1996; Basser and Pierpaoli, 1998; Basser and Jones, 2002). A grand average FA image was constructed by applying the structural transformation matrix to the FA images.

Fiber Tracking

Target and source regions were defined on the aligned grand average FA data, followed by minor manual editing for each subject on his FA images that contributed to the grand average (after registration to common coordinates, described above). The target comprised the midsagittal corpus callosum, divided geometrically into six regions of interest (Fig. 1) but guided by the callosal anatomical projections described by (Pandya and Seltzer, 1986). The fiber source was defined as two parallel parasagittal planes located 10 mm on either side of the midsagittal corpus callosum and extending across the entire brain. Identified fibers were required to pass through both sources to ensure identification of callosal fibers that extended to both hemispheres.

The target and source were then transformed into each subject's native coordinates using the inverse of the original warping transform (Woods *et al.*, 1998a,b) and the fiber tracking performed on native, unwarped DTI data for each of the callosal regions of interest separately. Fiber tracking was performed with the software distributed by Gerig *et al.* (2005) based on the method of Mori and colleagues (Mori and van Zijl, 2002; Xu *et al.*, 2002; Xue *et al.*, 1999). Fiber tracking parameters included white matter extraction threshold (minimum FA) of 0.17, minimum fiber length of 37.5 mm, maximum fiber length of 187.5 mm, fiber tracking threshold of 0.125 and maximum voxel-to-voxel coherence minimum transition smoothness threshold of 0.80 (~37° maximum deviation between voxels), with no limit on the number of fibers. The mean FA and ADC of each voxel comprising each fiber, for all fibers, were determined. After fiber detection the fiber locations were transformed back to common coordinates for display and further analysis (Fig. 2). For each callosal region the number of fibers, the mean fiber length, FA, ADC, and λ_1, λ_2, and λ_3 were determined. We refer hereafter to the fibers coursing through each of the six callosal regions as 'fiber bundles' following the Pandya and Selzer convention: prefrontal, premotor/precentral, postcentral, posterior parietal, superior temporal, and inferior temporal/occipital (Fig. 1).

Corpus Callosum Size

The area of the corpus callosum was identified on the midsagittal slice extracted from the SPGR data after alignment along the AC–PC and reslicing to isotropic voxels, but before any linear or nonlinear warping, that is, preserving each subject's native brain size. A semi-automated edge identification procedure with high interrater reliability was used to outline the corpus callosum (Schulte *et al.*, 2003). The callosal silhouette was rotated to a plane parallel to the inferior extremes of the rostrum anteriorly and splenium posteriorly (Sullivan *et al.*, 2002), and the height, length and total midsagittal callosal area determined.

Cognitive Testing

All subjects in the older (but not younger) group completed the conventional Stroop Color–Word Test (Stroop, 1935; Golden, 1978) as

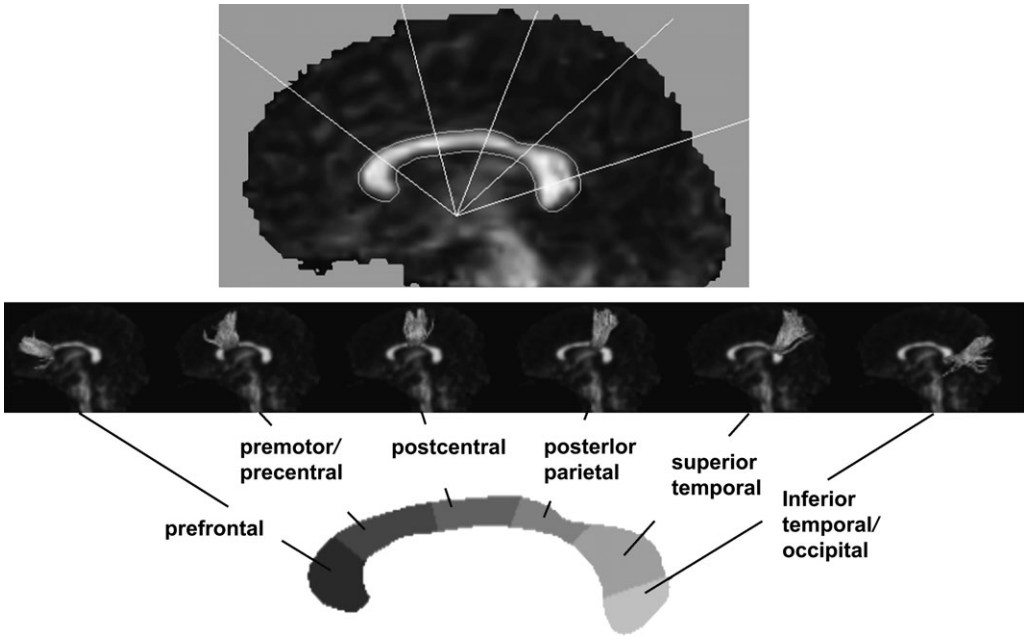

Figure 1. Midsagittal grand average FA image with callosal sector division lines superimposed. The divisions define the six callosal regions, which served as fiber bundle targets.

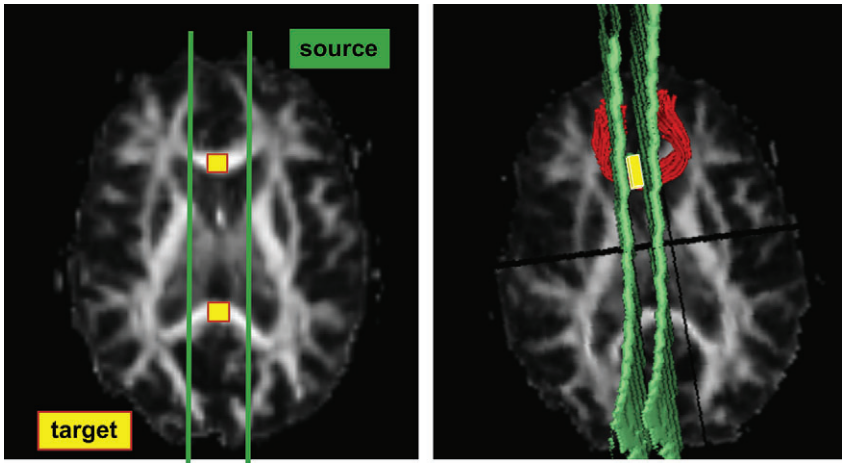

Figure 2. Left: nonlinearly aligned axial FA image from an individual subject with callosal target regions marked in yellow and bilateral fiber sources in green. Right: same subject's FA image, fiber sources and target, in native (unwarped) space, with one fiber bundle identified.

part of another protocol conducted contemporaneously with the current imaging study. For each of the three parts of the test, subjects were given 45 s to name, as quickly and accurately as possible, color swatches (Color), names of colors printed in black ink (Word), and names of colors printed in ink incongruent with the color name (CW). In addition to the number of words correctly read, the CW condition, a test of interference, was scored correcting for Color and Word reading performance and applying age corrections to raw scores: (CW) – [(Color × Word)/(Color + Word)].

Statistical Analysis

Four metrics of the DTI analysis were subjected to separate, two-group repeated measures analysis of variance (ANOVA) across six regionally defined fiber bundles: FA, ADC, fiber number and fiber length. Follow-up comparisons were based on within-subject and between-subject *t*-tests. Pearson product-moment correlations tested relations between Stroop test scores and DTI metrics, with the directional predictions that more words correctly named would correlate with higher FA, lower ADC, longer fiber length, or greater fiber number. Because of the small sample size, the correlations were not subjected to correction for multiple comparisons and must be considered exploratory.

Results

Fiber tracking examples of a younger and an older woman are presented in Figure 3, and group mean ± SEM values for FA, ADC, fiber length and fiber number are presented in Figure 4. For FA, the ANOVA revealed significant effects of group [$F(1,18) = 16.441$, $P = 0.0007$] and bundle [$F(5,90) = 114.86$, $P = 0.0001$], and a group × bundle interaction [$F(5,90) = 16.09$, $P = 0.0001$]. Together with follow-up paired comparisons, these results indicated that the older group had disproportionately low FA in the three frontal fiber bundles. The ANOVA for ADC revealed a complementary pattern to that of FA, with the older group having higher ADC than the younger group [group effect, $F(1,18) = 11.126$, $P = 0.0037$; bundle effects, $F(5,90) = 4.68$ $P = 0.0008$], notable in the two most anterior bundles [group × region interaction, $F(5,90) = 5.61$, $P = 0.0002$]. Although the overall difference in fiber length was not significant between the groups [$F(1,18) = 0.182$, $P = 0.67$], a bundle effect [$F(5,90) = 55.88$ $P = 0.0001$] together with a group × bundle interaction [$F(5,90) = 3.64$, $P = 0.0048$] and follow-up *t*-tests indicated that the older group had shorter fibers than the younger group in the most anterior callosal bundle alone. Overall, fewer fibers were identified in the older than younger group [$F(1,18) = 11.24$,

Figure 3. Six fiber bundles projected into common space for a younger and an older woman. The top two images are sagittal views and the bottom two are axial views. Red fibers are the most anterior (prefrontal) and green fibers are the most posterior (inferior temporal/occipital).

$P = 0.0035$] and there was regional variation in fiber numbers per bundle [$F(5,90) = 22.04$, $P = 0.0001$], but the group × bundle interaction was not significant [$F(5.90) = 0.889$, $P = 0.49$]. To test whether differences in fiber number could account for the age effects observed in FA and ADC, analyses of covariance (ANCOVAs) were conducted, using fiber number as the covariate. The same pattern of regional differences in FA and ADC observed with simple ANOVAs endured with ANCOVAs.

Fiber tract identification (Gerig *et al.*, 2005) is based on anisotropy measures, with criteria for minimal FA value, local curvature and local coherence, and provides location information. The concept of 'quantitative fiber tracking' examines quantitatively the diffusion characteristics of the voxels comprising the fibers. In addition to FA, ADC, which describes the amount of diffusion but has no orientational information, and the magnitude of each eigenvalue, which describes the amount

of diffusion in each of three orthogonal orientations, are assessed to provide information about the integrity of the identified fibers. These metrics describe the integrity of the fiber bundle along its entirety rather than merely where fibers cross the corpus callosum.

The diffusion tensor provides a description of an ellipsoid with three principal components or axes, λ_1, λ_2 and λ_3, such that a larger λ reflects greater diffusivity. λ_1 is the largest component (tensor eigenvalue) and serves to define the long axis of the ellipsoid. λ_2 and λ_3 are the shorter axes and contribute to the definition of the girth of the ellipsoid. The more that λ_1 exceeds λ_2 and λ_3, the greater the anisotropy, that is, the higher the FA; conversely, FA is lower when no λ predominates. In contrast to FA, ADC represents the average of all three λs. We examined the differential contribution of the three λs to ascertain how they contributed to the regional differences in FA using a two-factor repeated-measures ANOVA (Greenhouse–Geiser correction) for each callosal bundle for each group. Although the λ_1 was greater in the older than the younger group, this effect was small compared with that of λ_2 and λ_3, especially in the frontal bundles. A significant three-way interaction [$F(10,180) = 6.304$, $P = 0.0002$] indicated that diffusivity was disproportionately greater in the frontal than posterior bundles in the older than the younger group and that the groups differed especially in the magnitude of λ_2 and λ_3 of the prefrontal and premotor bundles (Fig. 5). In essence, the

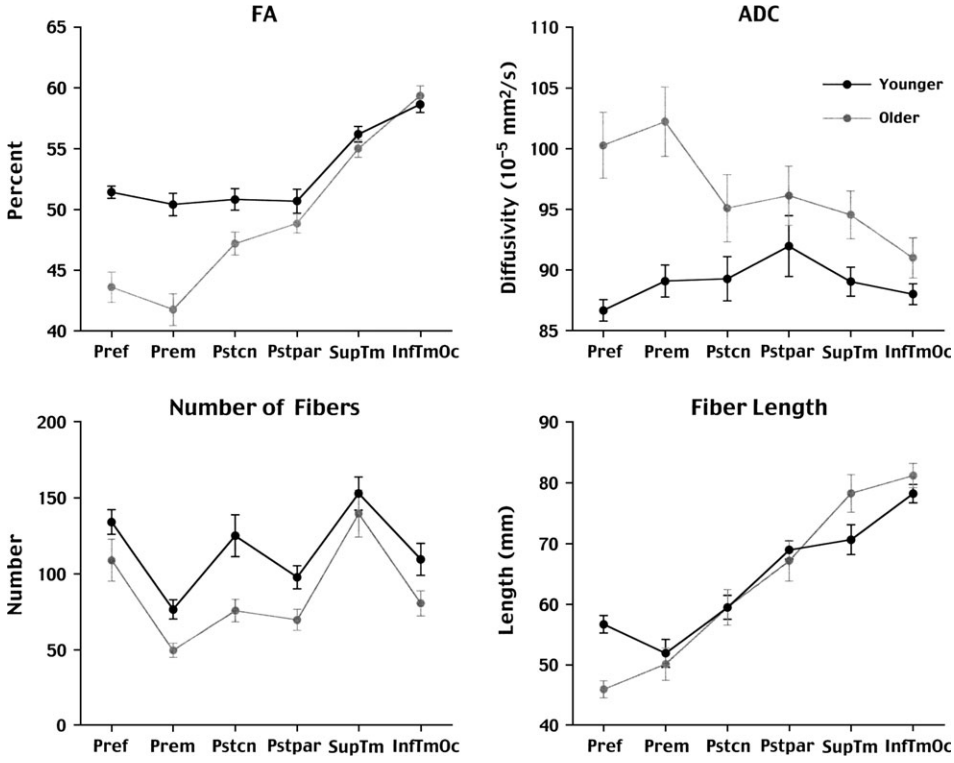

Figure 4. Mean ± SEM for FA, ADC, number of fibers, and fiber length across the six fiber bundles of the younger and older groups.

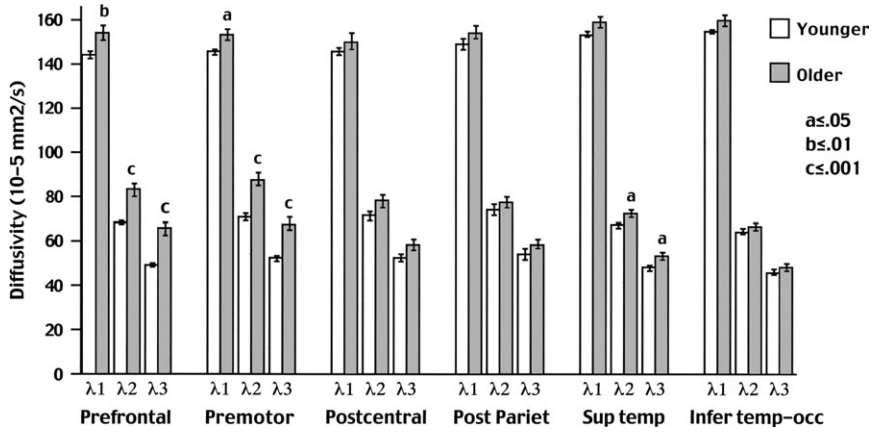

Figure 5. Mean ± SEM diffusivity for λ_1, λ_2, λ_3 across the six fiber bundles for the younger and older groups. Note the relative greater difference (older greater than younger) in diffusivity for λ_2 and λ_3 in the prefrontal and premotor fiber bundles.

tensor ellipsoids comprising the prefrontal and premotor fiber bundles were a little longer but substantially wider in the older than younger subjects.

Fiber tracking metrics were used in correlational analysis as predictors of output scores on the Stroop Color–Word Test in the older group only. Scatterplots of the significant correlations ($P \leq 0.05$, one-tailed) are presented in Figure 6. The most consistent correlations were between more words read in the simple word reading condition (W) and higher FA ($r = 0.59$, $P < 0.04$) or lower ADC ($r = -0.59$, $P < 0.04$) in the premotor/precentral callosal bundle. Additional correlations were present between this word reading condition and FA in the postcentral bundle ($r = 0.68$, $P < 0.02$), and numbers of fibers in the posterior parietal ($r = 0.60$, $P < 0.035$) and superior temporal ($r = 0.62$, $P < 0.03$) bundles. In the simple color naming condition (C), number of colors named correlated with fiber length in the superior temporal bundle ($r = 0.59$, $P < 0.04$). Although the formal interference score based on performance in the incongruent color–word condition (CW) did not correlate with any regional DTI metric, the raw output of words correctly read in the CW condition did correlate with fiber length in the postcentral bundle ($r = 0.62$, $P < 0.03$).

The potential influence of age on these DTI–Stroop correlations was examined by recalculating the correlations partialling out age. In all but one case, age did not endure as a significant unique predictor of performance over and above the contribution from the DTI measures ($P \leq 0.05$). The exception was for word reading, to which the FA measures made a stronger contribution (partial $F = 7.37$, $P = 0.0035$) than age (partial $F = 3.07$, $P = 0.0331$).

Finally, the effect of age was examined for conventional MRI measures of callosal morphology. Group comparisons revealed that the older group had a sagittal callosal silhouette that was significantly taller [$t(18) = 3.213$, $P < 0.005$] and tended to be longer [$t(18) = 1.790$, $P = 0.09$] than that of the younger group, but that the groups did not differ significantly in callosal area [younger mean = 592.3 ± 19.9mm^2; older mean = 566.5 ± 31.2mm^2; $t(18) = 0.698$ $P = 0.49$].

Discussion

This DTI tractography analysis used fiber targets comprising the midsagittal corpus callosum, divided into six regions based on known callosal anatomical projections connecting the two cerebral hemispheres (de Lacoste *et al.*, 1985; Pandya and Seltzer, 1986). Determination of FA and ADC for each voxel of each fiber identified revealed that the older subjects had lower FA, higher ADC and fewer fibers than younger subjects. These age differences were disproportionately greater for FA, ADC, and fiber length in frontal relative to posterior fiber bundles. Number of fibers identified with the study criteria did not show the age-related anteroposterior effect, and group differences in fiber numbers did not account for observed differences in FA or ADC. The age-related differences in DTI metrics provide validation for this quantitative fiber tracking approach and support the selective vulnerability of frontal white matter systems to normal aging as likely substrates of age-related declines in cognitive processes dependent on the integrity of interhemispheric circuitry linking prefrontal systems.

The sensitivity of DTI fiber tracking to detect age differences was clear when placed within the context of the conventional macrostructural MRI data, which yielded no age difference in overall size of the corpus callosum through which the fibers passed. Indeed, the only group differences detected with structural MRI herein were for callosal length and height, which we previously showed to be explained by age-associated ventricular expansion (Sullivan *et al.*, 2002; Pfefferbaum *et al.*, 2004). Prior MRI studies of callosal size report, at most, modest shrinkage of the midsagittal area (Driesen and Raz, 1995) that appear to accelerate in older age (Salat *et al.*, 1997).

The tensor-defined ellipsoids describing prefrontal and premotor fiber bundles were a little longer but substantially wider

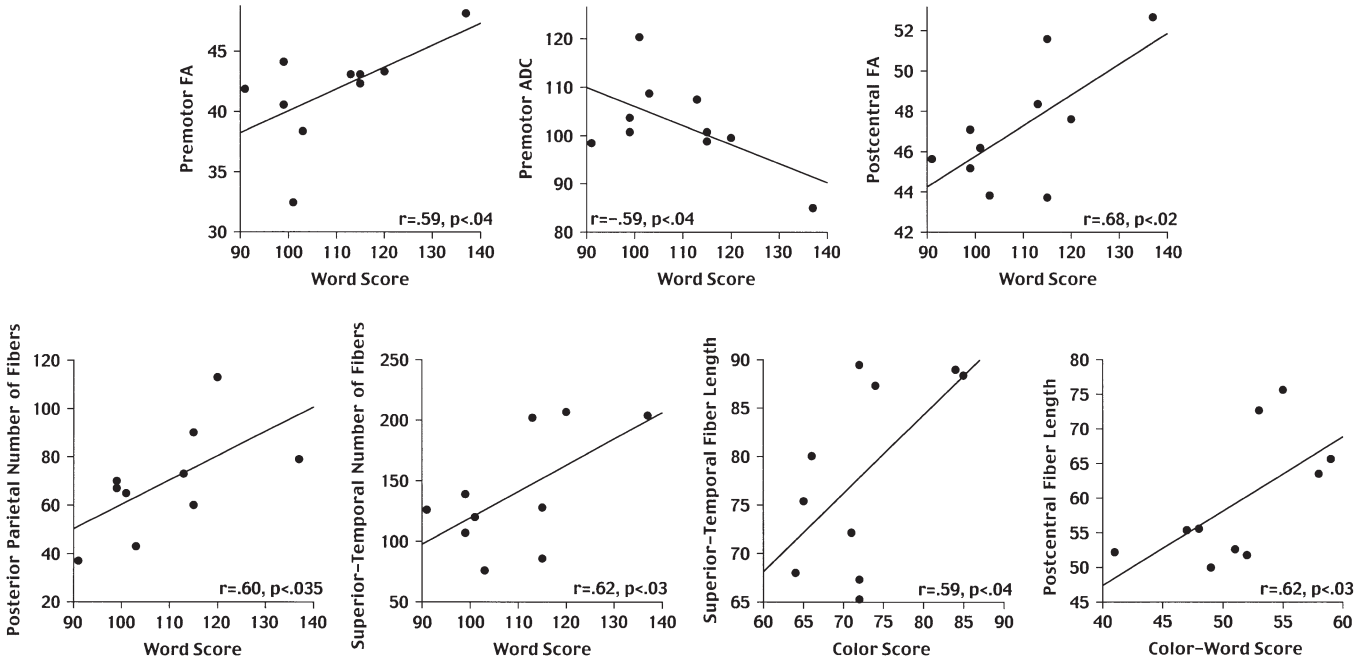

Figure 6. Correlations between conditions of the Stroop Color–Word Test and regional callosal DTI metrics.

in the older than younger subjects. The age-related difference in tensor ellipsoid shape together with the higher ADC is indicative of a greater presence of mobile water molecules characterizing fibers of older individuals. Whether this motility is more abundant in intracellular than extracellular spaces cannot currently be definitively discerned *in vivo*. It may, however, reflect age-related breakdown of myelin sheathing, trapping of fluid between thin or lysed sheathes and between fibers and bulbous swelling of oligodendrocytes (Peters *et al.*, 2001; Peters and Sethares, 2002, 2003).

The functional relevance of the regional fiber tracking DTI metrics was challenged with the Stroop Test. This task taps multiple component processes—including color perception, word reading, selective attention, and response inhibition (Cohen and Servan-Schreiber, 1992; Peterson *et al.*, 1999; Cabeza and Nyberg, 2000; Liotti *et al.*, 2000)—and multiple cortical processing sites but not necessarily transcallosal information exchange (Weekes and Zaidel, 1996; Funnell *et al.*, 2000; Belanger and Cimino, 2002). Bilateral distribution of processing, however, may enhance performance speed or accuracy, especially in older individuals. For example, functional imaging studies reveal that older healthy adults who perform well on lateralized tests of language, verbal or source memory, and GO/NOGO response inhibition tasks activate bilateral cortical regions (Cabeza, 2002; Cabeza *et al.*, 2002; Langenecker and Nielson, 2003), whereas younger healthy adults and older adults who perform poorly recruit unilateral brain regions (Cabeza, 2002; Cabeza *et al.*, 2002). We offer the possibility that poor bilateral recruitment by older subjects arises, at least in part, from degradation of callosal fibers, which may reduce the opportunity for bilateral recruitment.

Despite our small sample size, several correlations emerged, the most consistent were based on number of words read in the simple word reading condition, which correlated with higher anisotropy and lower diffusivity in the premotor/precentral callosal bundle as well as with higher anisotropy in the postcentral bundle and numbers of fibers in the superior and inferior temporal/parietal bundles. Similar correlations were observed in a longitudinal study of elderly men, for whom decline in Stroop word reading speed correlated with thinning of the callosal body (Sullivan *et al.*, 2002). Performance in the simple color naming condition correlated with fiber length in the superior temporal bundle, which extends to cortical sites involved in color naming (Chao and Martin, 1999; Peterson *et al.*, 1999). The incongruent color–word interference condition, which assesses selective attention and response inhibition, correlated with fiber length in the postcentral bundle, which may extend to parietal cortical attentional networks (Pujol *et al.*, 2001) involved in conflict monitoring (Fassbender *et al.*, 2004). Drawing on this posterior attentional system may be advantageous, given evidence that a ventral visual cortical processing stream subserves the inhibition of word reading, a requirement for good performance on the incongruent color–word task (Harrison *et al.*, 2005). It was surprising, however, that performance on this task was not also related to fiber tracking measures of callosal sectors connecting inferior frontal regions, given their contribution to response inhibition and inhibitory control (e.g. Rubia *et al.*, 2003; Herrmann *et al.*, 2005; Kemmotsu *et al.*, 2005; McDonald *et al.*, 2005). Perhaps use of a more challenging or selective task than the classical Stroop task but also requiring response inhibition (e.g. Schulte *et al.*, 2005) would yield predictable correlations between frontal callosal microstructural integrity and performance (cf. Stuss *et al.*, 1999). In summary, these correlations, distributed along the callosal body fiber bundles, support the likelihood that tractography output, while only a mathematical representation of underlying structure, is functionally meaningful. Further, the functional ramifications of age-related degradation of callosal white matter fibers may be detectable using challenging tasks in elderly subjects, even when they remain able to engage in useful bilateral activation.

The obvious candidate for enabling age-related recruitment of bilateral brain systems for high performance is the corpus callosum. In addition to providing a means for interhemispheric communication for sensory and motor integration (Gazzaniga, 1995), corpus callosum integrity may influence the allocation of resources when attentional or memory capacity is limited (Banich, 1998; Reuter-Lorenz and Stanczak, 2000; Zaidel and Iacoboni, 2003). Some have interpreted the bilateral pattern as evidence for decline in functional hemispheric laterality, arising from compromise of the callosum's capacity to inhibit participation of the hemisphere less suited to accomplish a task (Kinsbourne, 1974; Banich, 1998). The outcome can appear as 'dedifferentiation' of hemispheric function (Dolcos *et al.*, 2002). Given that age-related degradation of white matter is considered nonpathological, subtle compromise may actually enable bilateral engagement of the hemispheres (Buckner, 2004), but more substantial compromise may attenuate efficient interhemispheric information transfer. Thus, compensatory mechanisms must be in place to meet the challenge of difficult tasks (Buckner, 2004)—those requiring greater resources, especially from frontal sites (Anderson and Grady, 2001).

Although it is estimated that only ~2–3% of cortical sites are bilaterally distributed via the corpus callosum, ~93% of interhemispheric connections course through the corpus callosum (LaMantia and Rakic, 1990). The corpus callosum is thus the principal vehicle for information transfer between the hemispheres and a significant substrate to permit functional plasticity in compensation for damage arising from unilateral cortical lesions (Schwartz and Goldman-Rakic, 1990; Schwartz and Goldman-Rakic, 1991), induced transient 'lesions' from transcranial magnetic stimulation (Sack *et al.*, 2005) or deterioration associated with normal aging (Cabeza *et al.*, 2004). Selective disruption of frontally based fibers are likely structural substrates of age-related declines in cognitive processes dependent on functioning of the prefrontal circuitry (Raz *et al.*, 2004), and evidence from DTI studies is accruing in support of an anteroposterior gradient of degradation of age-related callosal, pericallosal and extracallosal white matter microstructure (for a review, see Sullivan and Pfefferbaum, 2005). Pericallosal fibers show striking signs of aging in the form of low anisotropy and high diffusivity (Pfefferbaum *et al.*, 2000b; Sullivan *et al.*, 2001; Bhagat and Beaulieu, 2004; Salat *et al.*, 2005) and may contribute to degradation of aging frontal callosal and subcortical systems. Further, frontal sites are under proportionately greater environmental than genetic control than are posterior regions, as evidenced in our study of twins revealing that the proportion of genetic to environmental contributions to FA was 3:1 for the splenium but only 1:1 for the genu (Pfefferbaum *et al.*, 2001).

Given the small samples and restricted neuropsychological assessment, this study has limitations for generalizability and for determination of brain structure–function relations. Further, the callosal sectors defining fiber bundles herein were

determined by grossly identifying sulcal markings on the averaged structural MRI data that corresponded to the six cortical target sites. Others have used cortical regions as fiber sources to define bundles coursing through the corpus callosum and could validate the uniqueness of a bundle with correlative data from pathology (Huang *et al.*, 2005). Our analysis provides an initial attempt at quantifying relevant brain white matter fiber bundles with possible functional significance.

The effects of normal adult aging are subtle, accrue insidiously and can be elusive to detection with conventional structural neuroimaging techniques. The growing body of DTI research substantiates its utility for *in vivo* detection of anteroposterior patterns of sparing and compromise of white matter integrity in normal aging. The predilection for age-related decline in anterior white matter fiber integrity may underlie the declining executive functioning common in groups of older yet healthy individuals (for reviews, see Raz, 1999; Buckner, 2004; Hedden and Gabrieli, 2004; Sullivan and Pfefferbaum, 2005). As an index of brain tissue quality, DTI permits examination of regional patterns of neural circuitry degeneration associated with aging and accessible with quantitative tractography. Future studies combining fiber tracking with DTI, high-resolution structural information from MRI, and functional MRI (fMRI) may provide precise delineations of fiber bundles that connect specific cortical sites for interhemispheric transfer of selective cognitive, sensory and motor processing.

Notes

This work was supported by NIH grants AA05965, AA10723, AA12388, and AG17919.

Address correspondence to Edith V. Sullivan, Department of Psychiatry and Behavioral Sciences, Stanford University School of Medicine, 401 Quarry Road, Stanford, CA 94305, USA. Email: edie@stanford.edu.

Funding to pay the Open Access publication charges for this article was provided by the National Institute of Health.

References

Aboitiz F, Rodriguez E, Olivares R, Zaidel E (1996) Age-related changes in fibre composition of the human corpus callosum: sex differences. Neuroreport 7:1761–1764.

Anderson ND, Grady CL (2001) Functional imaging in cognitively intact aged people. In: Functional neurobiology of aging (Hof PR, Mobbs CV, eds), pp. 211–225. San Diego, CA: Academic Press.

Arfanakis K, Cordes D, Haughton VM, Carew JD, Meyerand ME (2002) Independent component analysis applied to diffusion tensor MRI. Magn Reson Med 47:354–363.

Banich MT (1998) The missing link: the role of interhemispheric interaction in attentional processing. Brain Cogn 36:128–157.

Bartzokis G (2004) Age-related myelin breakdown: a developmental model of cognitive decline and Alzheimer's disease. Neurobiol Aging 25:5–18 (author reply 49–62).

Basser PJ (1998) Fiber-tractography via diffusion tensor MRI (DT-MRI). In: Proceedings of the International Society of Magnetic Resonance in Medicine, 6th meeting, p. 1226. Berkeley, CA: International Society of Magnetic Resonance in Medicine.

Basser PJ, Jones DK (2002) Diffusion-tensor MRI: theory, experimental design and data analysis — a technical review. NMR Biomed 15:456–467.

Basser PJ, Pierpaoli C (1996) Microstructural and physiological features of tissues elucidated by quantitative diffusion tensor MRI. J Magn Reson B 111:209–219.

Basser PJ, Pierpaoli C (1998) A simplified method to measure the diffusion tensor from seven MR images. Magn Reson Med 39:928–934.

Beaulieu C, Allen PS (1994) Water diffusion in the giant axon of the squid: implications for diffusion-weighted MRI of the nervous system. Magn Reson Med 32:579–583.

Belanger HG, Cimino CR (2002) The lateralized stroop: a meta-analysis and its implications for models of semantic processing. Brain Lang 83:384–402.

Bhagat YA, Beaulieu C (2004) Diffusion anisotropy in subcortical white matter and cortical gray matter: changes with aging and the role of CSF-suppression. J Magn Reson Imaging 20:216–227.

Bodammer N, Kaufmann J, Kanowski M, Tempelmann C (2004) Eddy current correction in diffusion-weighted imaging using pairs of images acquired with opposite diffusion gradient polarity. Magn Reson Med 51:188–193.

Buckner RL (2004) Memory and executive function in aging and AD: multiple factors that cause decline and reserve factors that compensate. Neuron 44:195–208.

Cabeza R (2002) Hemispheric asymmetry reduction in older adults: the HAROLD model. Psychol Aging 17:85–100.

Cabeza R, Nyberg L (2000) Imaging cognition. II. An empirical review of 275 PET and fMRI studies. J Cogn Neurosci 12:1–47.

Cabeza R, Anderson ND, Locantore JK, McIntosh AR (2002) Aging gracefully: compensatory brain activity in high-performing older adults. Neuroimage 17:1394–1402.

Cabeza R, Daselaar SM, Dolcos F, Prince SE, Budde M, Nyberg L (2004) Task-independent and task-specific age effects on brain activity during working memory, visual attention and episodic retrieval. Cereb Cortex 14:364–3675.

Chao LL, Martin A (1999) Cortical regions associated with perceiving, naming, and knowing about colors. J Cogn Neurosci 11:25–35.

Chen ZG, Li TQ, Hindmarsh T (2001) Diffusion tensor trace mapping in normal adult brain using single-shot EPI technique. A methodological study of the aging brain. Acta Radiol 42:447–458.

Chepuri NB, Yen YF, Burdette JH, Li H, Moody DM, Maldjian JA (2002) Diffusion anisotropy in the corpus callosum. Am J Neuroradiol 23:803–808.

Cohen JD, Servan-Schreiber D (1992) Context, cortex, and dopamine: a connectionist approach to behavior and biology in schizophrenia. Psychol Rev 99:45–77.

Conturo T, Lori N, Cull T, Akbudak E, Snyder A, Shimony J, McKinstry R, Burton H, Raichle M (1999) Tracking neuronal fiber pathways in the living human brain. Proc Natl Acad Sci USA 96:10422–104727.

de Lacoste M, Kirkpatrick J, Ross E (1985) Topography of the human corpus callosum. J Neuropathol Exp Neurol 44:578–591.

Dolcos F, Rice HJ, Cabeza R (2002) Hemispheric asymmetry and aging: right hemisphere decline or asymmetry reduction. Neurosci Biobehav Rev 26:819–825.

Driesen NR, Raz N (1995) The influence of sex, age, and handedness on corpus callosum morphology: a meta-analysis. Psychobiology 23:240–247.

Engelter ST, Provenzale JM, Petrella JR, DeLong DM, MacFall JR (2000) The effect of aging on the apparent diffusion coefficient of normal-appearing white matter. Am J Roentgenol 175:425–430.

Fassbende, C, Murphy K, Foxe JJ, Wylie GR, Javitt DC, Robertson IH, Garavan H (2004) A topography of executive functions and their interactions revealed by functional magnetic resonance imaging. Brain Res Cogn Brain Res 20:132–143.

Fenrich FR, Beaulieu C, Allen PS (2001) Relaxation times and microstructures. NMR Biomed 14:133–139.

Folstein MF, Folstein SE, McHugh PR (1975) Mini-mental state: a practical method for grading the cognitive state of patients for the clinician. J Psychiatr Res 12:189–198.

Funnell MG, Corballis PM, Gazzaniga MS (2000) Insights into the functional specificity of the human corpus callosum. Brain 123:920–926.

Gazzaniga MS (1995) Principles of human brain organization derived from split-brain studies. Neuron 14:217–228.

Gerig G, Corouge I, Vachet C, Krishnan KR, MacFall JR (2005) Quantitative analysis of diffusion properties of white matter fiber tracts: a validation study. In: 13th Proceedings of the International Society for Magnetic Resonance in Medicine, Miami, FL, Abstract no. 1337.

Glover GH, Lai S (1998) Self-navigated spiral fMRI: Interleaved versus single-shot. Magn Reson Med 39:361–368.
Golden C (1978) Stroop color and word test: a manual for clinical and experimental uses. Chicago, IL: Stoelling Co.
Harrison BJ, Shaw M, Yucel M, Purcell R, Brewer WJ, Strother SC, Egan GF, Olver JS, Nathan PJ, Pantelis C (2005) Functional connectivity during Stroop task performance. Neuroimage 24:181–191.
Head D, Buckner RL, Shimony JS, Williams LE, Akbudak E, Conturo TE, McAvoy M, Morris JC, Snyder AZ (2004) Differential vulnerability of anterior white matter in nondemented aging with minimal acceleration in dementia of the Alzheimer type: evidence from diffusion tensor imaging. Cereb Cortex 14:410–423.
Hedden T, Gabrieli JD (2004) Insights into the ageing mind: a view from cognitive neuroscience. Nat Rev Neurosci 5:87–96.
Helenius J, Soinne L, Perkio J, Salonen O, Kangasmaki A, Kaste M, Carano RA, Aronen HJ, Tatlisumak T (2002) Diffusion-weighted MR imaging in normal human brains in various age groups. Am J Neuroradiol 23:194–199.
Herrmann MJ, Plichta MM, Ehlis AC, Fallgatter AJ (2005) Optical topography during a Go–NoGo task assessed with multi-channel near-infrared spectroscopy. Behav Brain Res 160:135–140.
Huang H, Zhang J, Jiang H, Wakana S, Poetscher L, Miller MI, van Zijl PC, Hillis AE, Wytik R, Mori S (2005) DTI tractography based parcellation of white matter: application to the mid-sagittal morphology of corpus callosum. Neuroimage 26:195–205.
Jenkinson M (2003) A fast, automated, *N*-dimensional phase unwrapping algorithm. J Magn Reson Med 49:193–197.
Jones D, Simmons A, Williams S, Horsfield M (1999) Non-invasive assessment of axonal fiber connectivity in the human brain via diffusion tensor MRI. Magn Reson Med 42:37–41.
Kemmotsu N, Villalobos ME, Gaffrey MS, Courchesne E, Muller RA (2005) Activity and functional connectivity of inferior frontal cortex associated with response conflict. Brain Res Cogn Brain Res 24:335–342.
Kemper, TL (1994) Neuroanatomical and neuropathological changes during aging and dementia. In: Clinical neurology of aging (Albert ML, Knoefel JE, eds), pp. 3–67. New York: Oxford University Press.
Kinsbourne M (1974) Mechanisms of hemispheric interaction in man. In: Hemispheric disconnection and cerebral function (Kinsbourne M, Smith WL, eds), pp. 260–285. Springfield, IL: Thomas.
LaMantia AS, Rakic P (1990) Cytological and quantitative characteristics of four cerebral commissures in the rhesus monkey. J Comp Neurol 291:520–537.
Langenecker SA, Nielson KA (2003) Frontal recruitment during response inhibition in older adults replicated with fMRI. Neuroimage 20:1384–1392.
Lazar M, Alexander AL (2005) Bootstrap white matter tractography (BOOT-TRAC). Neuroimage 24:524–532.
Le Bihan D (2003) Looking into the functional architecture of the brain with diffusion MRI. Nat Rev Neurosci 4:469–480.
Lehericy S, Ducros M, Van de Moortele PF, Francois C, Thivard L, Poupon C, Swindale N, Ugurbil K, Kim DS (2004) Diffusion tensor fiber tracking shows distinct corticostriatal circuits in humans. Ann Neurol 55:522–529.
Liotti M, Woldorff MG, Perez R, Mayberg HS (2000) An ERP study of the temporal course of the Stroop color–word interference effect. Neuropsychologia 38:701–711.
Madden DJ, Whiting WL, Huettel SA, White LE, MacFall JR, Provenzale JM (2004) Diffusion tensor imaging of adult age differences in cerebral white matter: relation to response time. Neuroimage 21:1174–1181.
Marner L, Nyengaard JR, Tang Y, Pakkenberg B (2003) Marked loss of myelinated nerve fibers in the human brain with age. J Comp Neurol 462:144–152.
Masutani Y, Aoki S, Abe O, Hayashi N, Otomo K (2003) MR diffusion tensor imaging: recent advance and new techniques for diffusion tensor visualization. Eur J Radiol 46:53–66.
Mattis S (1988) Dementia rating scale (DRS) professional manual. Odessa, FL: Psychological Assessment Resources, Inc.
McDonald CR, Delis DC, Norman MA, Wetter, SR, Tecoma ES, Iragui VJ (2005) Response inhibition and set shifting in patients with frontal lobe epilepsy or temporal lobe epilepsy. Epilepsy Behav (in press).
Meier-Ruge W, Ulrich J, Bruhlmann M, Meier E (1992) Age-related white matter atrophy in the human brain. Ann N Y Acad Sci 673:260–269.
Mori S, Kaufmann WE, Davatzikos C, Stieltjes B, Amodei L, Fredericksen K, Pearlson GD, Melhem, ER, Solaiyappan M, Raymond GV, Moser HW, van Zijl PC (2002) Imaging cortical association tracts in the human brain using diffusion-tensor-based axonal tracking. Magn Reson Med 47:215–223.
Mori S, van Zijl PC (2002) Fiber tracking: principles and strategies — a technical review. NMR Biomed 15:468–480.
Moseley ME, Cohen Y, Kucharczyk J, Mintorovitch J, Asgari HS, Wendland MF, Tsuruda J, Norman D (1990) Diffusion-weighted MR imaging of anisotropic water diffusion in cat central nervous system. Radiology 176:439–445.
Naganawa S, Sato K, Katagiri T, Mimura T, Ishigaki T (2003) Regional ADC values of the normal brain: differences due to age, gender, and laterality. Eur Radiol 13:6–11.
Neeman M, Freyer JP, Sillerud LO (1991) A simple method for obtaining cross-term-free images for diffusion anisotropy studies in NMR microimaging. Magn Reson Med 21:138–143.
O'Sullivan M, Jones D, Summers P, Morris R, Williams S, Markus H (2001) Evidence for cortical 'disconnection' as a mechanism of age-related cognitive decline. Neurology 57:632–638.
Pajevic S, Aldroubi A, Basser PJ (2002) A continuous tensor field approximation of discrete DT-MRI data for extracting microstructural and architectural features of tissue. J Magn Reson 154:85–100.
Pandya DN, Seltzer B (1986) The topography of commissural fibers. In: Two hemispheres — one brain: functions of the corpus callosum (Lepore F, Ptito M, Jasper HH, eds), pp. 47–74. New York: Alan R. Liss.
Peters A, Sethares,C (2002) Aging and the myelinated fibers in prefrontal cortex and corpus callosum of the monkey. J Comp Neurol 442:277–291.
Peters A, Sethares C (2003) Is there remyelination during aging of the primate central nervous system? J Comp Neurol 460:238–254.
Peters A, Sethares C, Killiany RJ (2001) Effects of age on the thickness of myelin sheaths in monkey primary visual cortex. J Comp Neurol 435:241–248.
Peterson BS, Skudlarski P, Gatenby JC, Zhang H, Anderson AW, Gore JC (1999) An fMRI study of Stroop word–color interference: evidence for cingulate subregions subserving multiple distributed attentional systems. Biol Psychiatry 45:1237–1258.
Pfefferbaum A, Sullivan EV (2003) Increased brain white matter diffusivity in normal adult aging: relationship to anisotropy and partial voluming. Magn Reson Med 49:953–961.
Pfefferbaum A, Sullivan EV (2005a) Diffusion MR imaging in neuropsychiatry and aging. In: Clinical MR neuroimaging: diffusion, perfusion and spectroscopy (Gillard J, Waldman A, Barker P, eds), pp. 558–578. Cambridge: Cambridge University Press.
Pfefferbaum A, Sullivan EV (2005b) Disruption of brain white matter microstructure by excessive intracellular and extracellular fluid in alcoholism: evidence from diffusion tensor imaging. Neuropsychopharmacology 30:423–432.
Pfefferbaum A, Lim KO, Desmond J, Sullivan EV (1996) Thinning of the corpus callosum in older alcoholic men: a magnetic resonance imaging study. Alc Clin Exp Research 20:752–757.
Pfefferbaum A, Sullivan EV, Rosenbloom MJ, Mathalon DH, Lim KO (1998) A controlled study of cortical gray matter and ventricular changes in alcoholic men over a five year interval. Arch Gen Psychiatry 55:905–912.
Pfefferbaum A, Sullivan EV, Hedehus M, Adalsteinsson E, Lim KO, Moseley M (2000a) *In vivo* detection and functional correlates of white matter microstructural disruption in chronic alcoholism. Alc Clin Exp Research 24:1214–1221.
Pfefferbaum A, Sullivan EV, Hedehus M, Lim KO, Adalsteinsson E, Moseley M (2000b) Age-related decline in brain white matter anisotropy measured with spatially corrected echo-planar diffusion tensor imaging. Magn Reson Med 44:259–268.
Pfefferbaum A, Sullivan EV, Swan GE, Carmelli D (2000c) Brain structure in men remains highly heritable in the seventh and eighth decades of life. Neurobiol Aging 21:63–74.

Pfefferbaum A, Sullivan EV, Carmelli D (2001) Genetic regulation of regional microstructure of the corpus callosum in late life. Neuroreport 12:1677–1681.
Pfefferbaum A, Sullivan EV, Carmelli D (2004) Morphological changes in aging brain structures are differentially affected by time-linked environmental influences despite strong genetic stability. Neurobiol Aging 25:175–183.
Pfefferbaum A, Adalsteinsson E, Sullivan EV (2005) Frontal circuitry degradation marks healthy adult aging: evidence from diffusion tensor imaging. Neuroimage 26:891–899.
Pfeuffer J, Van de Moortele PF, Ugurbil K, Hu X, Glover GH (2002) Correction of physiologically induced global off-resonance effects in dynamic echo-planar and spiral functional imaging. Magn Reson Med 47:344–353.
Pierpaoli C, Basser PJ (1996) Towards a quantitative assessment of diffusion anisotropy. Magn Reson Med 36:893–906.
Pujol J, Vendrell P, Deus J, Junque C, Bello J, Marti-Vilalta JL, Capdevila A (2001) The effect of medial frontal and posterior parietal demyelinating lesions on stroop interference. Neuroimage 13:68–75.
Raz N (1999) Aging of the brain and its impact on cognitive performance: integration of structural and functional findings. In: Handbook of aging and cognition II (Craik FIM, Salthouse TA, eds), pp. 1–90. Mahwah, NJ: Erlbaum.
Raz N, Gunning-Dixon F, Head D, Rodrigue K, Williamson A, Acker J (2004) Aging, sexual dimorphism, and hemispheric asymmetry of the cerebral cortex: replicability of regional differences in volume. Neurobiol Aging 25:377–396.
Raz N, Lindenberger U, Rodrigue KM, Kennedy KM, Head D, Williamson A, Dahle C, Gerstorf D, Acker JD (2005) Regional brain changes in aging healthy adults: general trends, individual differences, and modifiers. Cereb Cortex (in press).
Resnick SM, Pham DL, Kraut MA, Zonderman AB, Davatzikos C (2003) Longitudinal magnetic resonance imaging studies of older adults: a shrinking brain. J Neurosci 23:3295–301.
Reuter-Lorenz PA, Stanczak L (2000) Differential effects of aging on the functions of the corpus callosum. Developmental Neuropsychology 18:113–137.
Rubia K, Smith AB, Brammer MJ, Taylor E (2003) Right inferior prefrontal cortex mediates response inhibition while mesial prefrontal cortex is responsible for error detection. Neuroimage 20:351–358.
Sack AT, Camprodon JA, Pascual-Leone A, Goebel R (2005) The dynamics of interhemispheric compensatory processes in mental imagery. Science 308:702–704.
Salat D, Ward A, Kaye JA, Janowsky JS (1997) Sex differences in the corpus callosum with aging. Neurobiol Aging 18:191–197.
Salat DH, Tuch DS, Greve DN, van der Kouwe AJW, Hevelone ND, Zaleta AK, Rosen BR, Fischl B, Corkin S, Rosas HD, Dale AM (2005) Age-related alterations in white matter microstructure measured by diffusion tensor imaging. Neurobiol Aging 26:1215–1227.
Schulte T, Pfefferbaum A, Sullivan EV (2003) Parallel interhemispheric processing in aging and alcoholism: Relation to corpus callosum size. Neuropsychologia 42:257–271.
Schulte T, Müller-Oehring EM, Rosenbloom MJ, Pfefferbaum A, Sullivan EV (2005) Differential effect of HIV infection and alcoholism on conflict processing, attentional allocation, and perceptual load: evidence from a Stroop match-to-sample task. Biol Psychiatry 57:67–75.
Schwartz ML, Goldman-Rakic P (1990) Development and plasticity of the primate cerebral cortex. Clin Perinatol 17:83–102.
Schwartz ML, Goldman-Rakic PS (1991) Prenatal specification of callosal connections in rhesus monkey. J Comp Neurol 307:144–162.
Sehy JV, Ackerman JJ, Neil JJ (2002) Evidence that both fast and slow water ADC components arise from intracellular space. Magn Reson Med 48:765–770.
Silva MD, Omae T, Helmer KG, Li F, Fisher M, Sotak CH (2002) Separating changes in the intra- and extracellular water apparent diffusion coefficient following focal cerebral ischemia in the rat brain. Magn Reson Med 48:826–837.
Stieltjes B, Kaufmann WE, van Zijl PC, Fredericksen K, Pearlson GD, Solaiyappan M, Mori S (2001) Diffusion tensor imaging and axonal tracking in the human brainstem. Neuroimage 14:723–735.
Stroop JR (1935) Studies of interference in serial verbal reactions. J Exp Psychol 18:643–662.
Stuss DT, Toth JP, Franchi D, Alexander MP, Tipper S, Craik FI (1999) Dissociation of attentional processes in patients with focal frontal and posterior lesions. Neuropsychologia 37:1005–1027.
Sullivan EV, Pfefferbaum A (2005) Diffusion tensor imaging and aging. Neurosci Biobehav Rev (in press).
Sullivan EV, Adalsteinsson E, Hedehus M, Ju C, Moseley M, Lim KO, Pfefferbaum A (2001) Equivalent disruption of regional white matter microstructure in aging healthy men and women. Neuroreport 12:99–104.
Sullivan EV, Pfefferbaum A, Adalsteinsson E, Swan GE, Carmelli D (2002) Differential rates of regional change in callosal and ventricular size: a 4-year longitudinal MRI study of elderly men. Cereb Cortex 12:438–445.
Tang CY, Lu D, Wei TC, Spiegel J, Atlas SW, Buchsbaum MS (1997) Image processing techniques for the eigenvectors of the diffusion tensor (abs). International Society for Magnetic Resonance in Medicine, 5th meeting, 2054.
Waxman SG, Kocsis JD, Stys PK (1995) The axon: structure, function and pathophysiology. New York: Oxford University Press.
Weekes NY, Zaidel E (1996) The effects of procedural variations on lateralized Stroop effects. Brain Cogn 31:308–330.
Woods R, Grafton S, Holmes C, Cherry S, Mazziotta J (1998a) Automated image registration. I. General methods and intrasubject, intramodality validation. J Comput Assist Tomogr 22:139–152.
Woods RP, Grafton ST, Watson JD, Sicotte NL, Mazziotta JC (1998b) Automated image registration. II. Intersubject validation of linear and nonlinear models. J Comput Assist Tomogr 22:153–165.
Xu D, Mori S, Solaiyappan M, van Zijl PC, Davatzikos C (2002) A framework for callosal fiber distribution analysis. Neuroimage 17:1131–1143.
Xue R, van Zijl PC, Crain BJ, Solaiyappan M, Mori S (1999) In vivo three-dimensional reconstruction of rat brain axonal projections by diffusion tensor imaging. Magn Reson Med 42:1123–1127.
Zaidel E, Iacoboni M (2003) The parallel brain: the cognitive neuroscience of the corpus callosum. Cambridge, MA: The MIT Press.